PROCEEDINGS OF SCIENCE

Performance of the Pacific Ocean Neutrino Experiment

Jean Pierre Twagirayezu,[a,*] Hans Niederhausen,[a] Stephen Sclafani,[b] Nathan Whitehorn,[a] Mehr Nisa,[a] Shiqi Yu[a] and Robert Halliday[a] for the P-ONE Collaboration

[a] *Michigan State University, East Lansing, USA*
[b] *Drexel University, Philadelphia, USA*

E-mail: twagiray@msu.edu.edu

The Pacific Ocean Neutrino Experiment (P-ONE) is a proposed undersea neutrino detector in the northern Pacific near the British Columbia-Washington maritime boundary, with pathfinder instrumentation already deployed. P-ONE will consist of 1400 digital optical modules distributed across 70 strings. By deploying in a deep-sea environment, the scattering of Cherenkov photons is reduced relative to experiments in glacial ice, allowing event resolutions at or below a tenth of a degree. In this poster, we present and evaluate using Monte Carlo simulations a track reconstruction method that is based on a maximum likelihood method. Recorded light pulses are evaluated using pre-computed arrival time distributions of Cherenkov photons at optical modules as functions of track parameters. The corresponding angular resolution of the detector, when combined with the anticipated neutrino effective area, can be used to estimate the discovery potential, the flux needed to discover a point source of astrophysical neutrinos with P-ONE.

38th International Cosmic Ray Conference (ICRC2023)
26 July - 3 August, 2023
Nagoya, Japan

ICRC2023
38th International Cosmic Ray Conference
The Astroparticle Physics Conference

*Speaker

PoS(ICRC2023)1175

1. The Pacific Ocean Neutrino Experiment

The Pacific Ocean Neutrino Experiment (P-ONE) is a next-generation cubic kilometer-scale neutrino telescope in the deep Pacific Ocean off the coast of Vancouver Island, British Columbia [1]. The telescope aims to detect neutrinos of astrophysical origin, complementing other existing or under-construction neutrino telescopes [2, 3]. The detector will be deployed in the Cascadia Basin region, located 2600 meters below sea level [1]. P-ONE will greatly benefit from the existing deep-sea infrastructure of Ocean Networks Canada (ONC) [1] utilizing its capabilities for construction, deployment, power, and data communication. In collaboration with Ocean Networks Canada, P-ONE deployed STRAW in 2018 to measure the optical properties and backgrounds of the Cascadia Basin [4]. In deep-sea environments, the scattering of Cherenkov light is of the order of 100 m scattering length, providing good timing resolution [5]; this will enable event reconstruction with an excellent angular resolution and hence good capability to point back to the sources of astrophysical neutrinos.

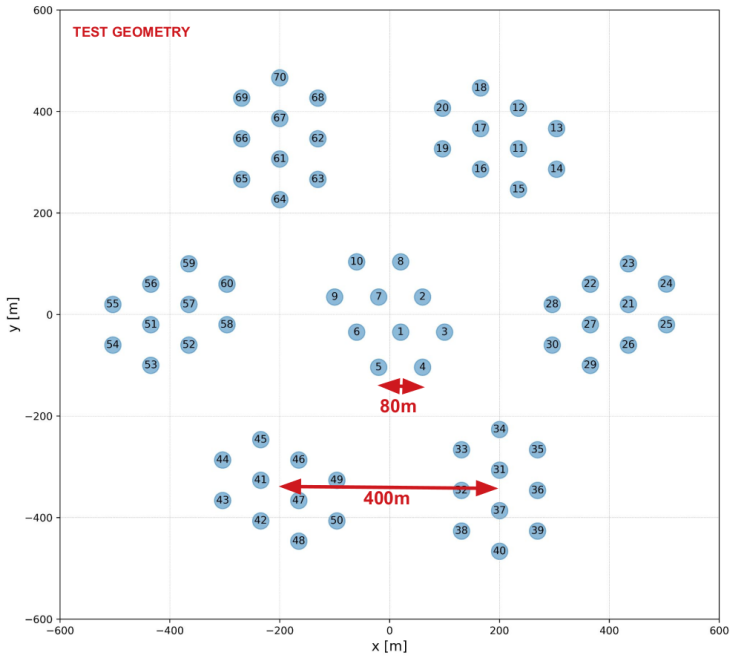

Figure 1: Top view of the simulated full 70-string P-ONE reference geometry used in this study. The string-to-string and cluster-to-cluster spacings are under optimization [6].

2. P-ONE Monte Carlo Simulation

In this work, we use a detailed Monte Carlo simulation to estimate event reconstruction performance and neutrino effective area, characterizing the P-ONE detector performance capabilities.

Detector Geometry The P-ONE detector would be deployed in modules, and a single module will be 10 vertical mooring lines, each 1 km long, consisting 20 P-ONE Optical Modules

(P-OMs) [7] per string at a vertical spacing of 50 meters [1]. Each P-OM will contain 16 photomultiplier tubes (PMTs) [5]. The Monte Carlo simulation used for this initial study uses the reference geometry shown in Fig. 1. The array has lines spaced by 80 meters within clusters and a 400-meter inter-cluster spacing (center-to-center). An ongoing effort is underway to optimize the geometry [6] for the string spacing and cluster spacing, which affect the sensitivity of the detector to astrophysical neutrino sources through both the angular resolution and the geometric volume of the detector.

Event Simulation The events simulated in this study were generated based on the methods developed for existing gigaton-volume neutrino detectors. The simulation workflow starts with simulating muon or neutrino events, then the propagation of secondary particles and Cherenkov photons in the detector medium, followed by detector response simulation, including noise and trigger simulation [8]. The Monte Carlo simulation in this study used the IceTray software framework [8]. We used MuonGun to simulate muon events with energy from 100 GeV to 1 PeV following E_{μ}^{-1}. Neutrino event simulation was performed using LeptonInjector [9] with energy ranging from 1 TeV to 10 PeV on an E_{ν}^{-1} spectrum, and have been re-weighted by LeptonWeghter [9]. We used PROPOSAL [10] for muon propagation through the detector medium. The photon propagation through the detector medium was done using CLSim [11], which takes into account the optical properties (scattering and absorption) of the Cascadia Basin water [4]. The detector hardware simulation used P-ONE specific software and assuming a baseline noise rate of 10 kHz [4]. Performance under variable rates of noise due to bioluminescence will be studied in the future.

3. Likelihood Reconstruction

Following standard maximum likelihood reconstruction techniques used by AMANDA [12] and later refined by IceCube [13], we have developed a likelihood-based reconstruction algorithm to determine the trajectory of a muon passing through the P-ONE detector. For each P-OM i that recorded light during the event, the data $\boldsymbol{t_i} = \{t_{ij}\}$ consists of the time stamps t_{ij} of the corresponding light pulses. The trajectory $\boldsymbol{x}(t)$, the position of the muon as a function of time, is parameterized using 5 parameters: the location $\boldsymbol{x_0} = (x_0, y_0, z_0)$ of the muon at some arbitrary time t_0, and the direction of the track $\boldsymbol{\theta} = (\theta, \phi)$. The zenith angle θ and azimuthal angle ϕ mark the origin of the muon in the sky and are the parameters of interest of our reconstruction algorithm.

Likelihood Function For a given track hypothesis $\boldsymbol{\Theta} = (\boldsymbol{x_0}, \boldsymbol{\theta})$ and any timestamp t_{ij}, we compute the residual time $t_{ij}^{res} = t_{ij} - t_i^{geo}(\boldsymbol{\Theta})$ at P-OM i following the geometrical formulae discussed in [12] while taking into account that the detector medium is ocean water instead of ice. At each P-OM, the distribution of residual times can be described using a two-component mixture model, consisting of a uniform probability density function (pdf), $f_b(t^{res})$, that accounts for detector noise, and a non-parametric arrival time distribution, $f_s(t^{res} \mid \boldsymbol{\Theta})$, that characterize the propagation of a photon from the track $\boldsymbol{\Theta}$ to the receiving P-OM through water. The full likelihood function reads

$$\log \mathcal{L}\left(\boldsymbol{\Theta} \mid \boldsymbol{t^{res}}\right) = \sum_i \left\{ \sum_j \log\left[p_i^s f_s\left(t_{ij}^{res} \mid \boldsymbol{\Theta}\right) + p_i^b f_b\left(t_{ij}^{res}\right)\right]\right\} \tag{1}$$

The mixture probabilities $p_i^s = 1 - p_i^b = 1 - q_b/q_i^{tot}$ are easily determined from the expected noise q_b and the measured total charge q_i^{tot} at P-OM i. The best-fit parameters $\hat{\mathbf{\Theta}}$ correspond to the global maximum of Eq. (1).

Residual Time PDF The performance of maximum likelihood methods hinges on the accuracy of the assumed likelihood model. Here, we derive the residual time pdfs $f_s(t^{res} \mid \mathbf{\Theta})$ from large-scale simulations of muons with varying energies and random trajectories through the P-ONE detector using the simulation framework described in Sec. 2. Specifically, we inject muons with random orientations within a volume that is slightly larger than that of the instrumented volume (60 m padding). For each muon, we tabulate the residual times of the photon pulses t_{ij}^{res} as a function of the distance $d_i(\mathbf{\Theta})$ that a photon would travel between its emission point on the track and the receiving P-OM i. We then approximate $f_s\left(t^{res} \mid \mathbf{\Theta}\right) \approx f_s\left(t^{res} \mid d(\mathbf{\Theta})\right)$ and construct the function on the RHS numerically by interpolating the corresponding 2D histogram using a non-parametric B-spline interpolation technique [14]. An example is shown in Fig. 2 (left) demonstrating that the B-spline representation of $f_s\left(t^{res} \mid d(\mathbf{\Theta})\right)$ evaluated at $d = 30$m matches well with the recorded photon arrival times at that distance.

Numerical Optimization Correctly identifying $\hat{\mathbf{\Theta}}$ is challenging because it requires globally optimizing a non-linear likelihood function in a five-dimensional parameter space. In addition, due to the low scattering coefficient in ocean water, the correct solutions correspond to very narrow minima in the negative log-likelihood space and are therefore easily missed. We address the latter issue by convolving the B-splines PDF [14, 15] with a Gaussian distribution, which, as a function of the Gaussian variance, broadens the likelihood minima. We perform a series of Gaussian-convolved likelihood optimizations starting with $\sigma = 35$ ns (most broadening) and ending with $\sigma = 0$ ns (no broadening). Each optimization uses starting values (seed) taken from the previous solution. The very first fit ($\sigma = 35$ ns) is started from the result of a simple LineFit method [16]. This Gaussian-convolved iterative fitting method is visualized in Fig. 2 (right). Each minimization is performed using the SIMPLEX algorithm [17]. At present, we do not have a method that guarantees global convergence. However, when studying the reconstruction performance on simulated muons, we can already approximate global convergence by using the true values of the track trajectory as a seed to a single likelihood optimization without convolution.

Angular Resolution To evaluate the performance of our reconstruction method, we again use simulated muons (cf. Sec. 2) with muon energies distributed as $\propto E^{-1}$ and random trajectories through the P-ONE detector. We reconstruct these muons using the algorithm described before. Specifically, we reconstruct each event twice, once using the Gaussian-convolved iterative likelihood fit and once using the true values $\mathbf{\Theta}$ as a seed. Comparisons between the likelihood values at the respective solutions reveal that the ones found by the truth-seeded fit generally have values that are smaller or equal to the ones obtained with the Gaussian-convolved iterative fit. Hence, we consider the truth-seeded fits as representative of the performance that will be achievable in the future, once the global convergence has been further optimized. To quantify the accuracy of the reconstruction we use the angular distance, or opening angle, between the true trajectory $\mathbf{\Theta}$ and the estimated one $\hat{\mathbf{\Theta}}$, as a metric. Figure (3a) shows the median angular resolution as a function of the muon energy

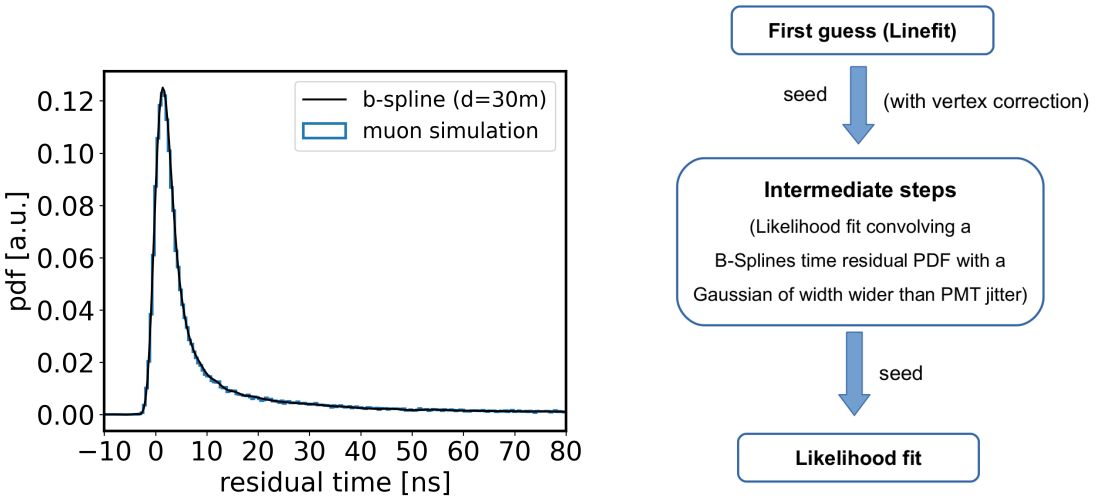

(a) (b)

Figure 2: (a) Distribution of residual times recorded at a distance of 30 m from the emission point on the muon track (blue. The b-spline representation (black) matches the data well. **(b) Overview over the Gaussian-convolved iterative fitting method**. Four intermediate likelihood fits are performed using B-splines convolved successively with Gaussians of width 35 ns, 20 ns, 10 ns, and 5 ns.

for muons with various minimum track lengths. Here, the length of the visible track in the detector is computed from the Gaussian-convolved iterative fit. Large values arise when long tracks are well reconstructed. Resolutions are given for both optimization strategies, Gaussian-convolutions (solid) and truth-seeding (dashed). As expected, the accuracy improves with the energy of the muon and the estimated length of its track in the detector. Based on the truth-seeded solutions, we conclude that P-ONE should be able to reach an angular resolution with > 700 m muon tracks of $\sim 0.1^\circ$ at 1 TeV, which improves to $\sim 0.05^\circ$ at 1 PeV. These values are a factor of ~ 4 better than those currently achieved by IceCube (blue solid line) [13]. The one-dimensional distribution of the opening angle is shown in Fig. (3b) for muon tracks with length larger than 700 m, for both the Gaussian-convolved iterative fits (dashed) and the truth-seeded method (solid). Around 74% (63%) of events with track lengths greater than 700 m have opening angles less than 0.1° in the truth-seeded (Gaussian-convolved iterations) method. Ongoing work on global convergence is expected to reduce the population of misreconstructed events for the Gaussian-convolved iterations-based method.

Effective Area To assess the performance of P-ONE in terms of effective area, neutrino events were simulated using LeptonInjector following an energy spectrum E_ν^{-1}, and later re-weighted to a signal spectrum of E_ν^{-2} using LeptonWeighter [9]. Neutrino effective area generally is calculated as

$$A_{\text{eff}} = \frac{\pi r_{\text{gen}}^2 \Omega_{\text{gen}} \sum_i \frac{p_{\text{int},i}}{N p_{\text{gen},i}}}{\Omega \, \Delta E} \tag{2}$$

where ΔE is the range of energies being summed over, Ω_{gen} the solid angle over which the simu-

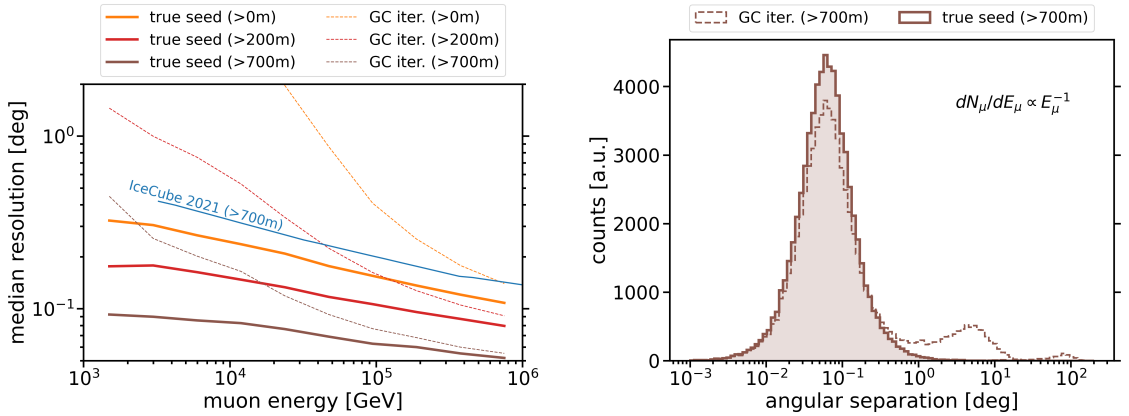

(a) **(b)**

Figure 3: (a) Median angular resolution as a function of muon energy for different selections based on the estimated visible length of the muon track in the detector for truth-seeded fits (true seed) and Gaussian-convolved iterations (GC iter.). The IceCube angular resolution for muon tracks of at least 700 m [13] is also shown for comparison (blue). **(b) Distribution of angular separation** between the true direction of the muon and the reconstructed one for estimated visible track lengths of at least 700 m using simulated muons with energies following E_μ^{-1}. Both figures show results obtained using the Gaussian-convolved iterative reconstruction (dashed lines) and the truth-seeded one (solid lines).

lation was generated, Ω the solid angle for which the effective area is being computed, $p_{\text{gen},i}$ and $p_{\text{int},i}$ are generation and interaction probabilities of the individual event respectively and N is the number of generated events [18].

Anticipated Point Source Sensitivity Both effective area and angular resolution performance are key ingredients to estimate the sensitivity to neutrino sources. The simulated 70-string configuration has an effective area comparable to that of IceCube [19] as shown in Fig. (4). With similar geometric size the analysis-level effective area should also be similar to IceCube effective area, although a full event selection chain has not yet been implemented for P-ONE. Initial studies show that the angular resolution will be potentially much better with improved event selection, Fig. (3). As the ability to detect point sources scales proportionally with the angular resolution, P-ONE should be several times more sensitive to sources than IceCube, although a full estimate is not included in this work. Detailed studies are underway to refine our estimate of the sensitivity of P-ONE to astrophysical sources of neutrinos.

4. Summary and Outlook

We have used a Monte Carlo simulation of the P-ONE detector to study muon track reconstruction. In the current results, using the preliminary P-ONE likelihood reconstruction, more than 60% of events with visible track length greater than 700 m have an opening angle less than 0.1 degrees. The combination of detector size comparable to existing observatories (Figure (4)) with significantly improved angular resolution (Figure (3b)) provides potentially superior sensitivity to astrophysical sources of high-energy neutrinos. In addition, P-ONE's location in the northern Pacific Ocean will

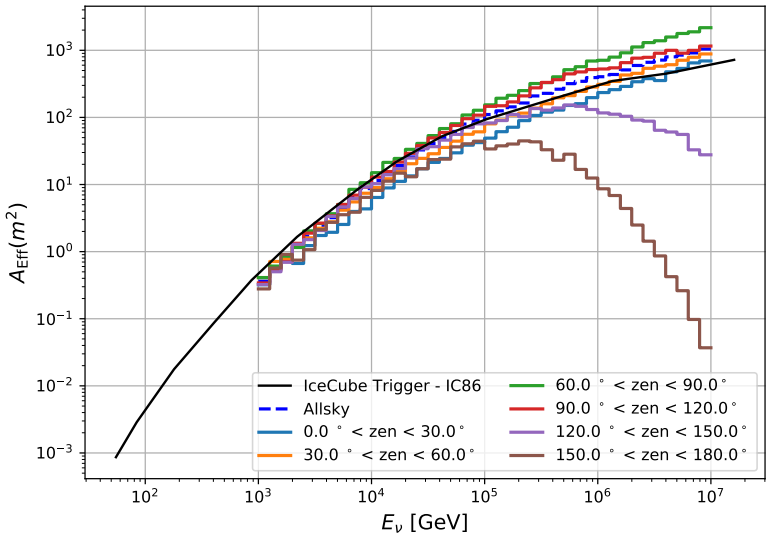

Figure 4: Effective area of the simulated P-ONE reference geometry as a function of neutrino energy, for different zenith angle bands at trigger level. The effects of Earth absorption on neutrinos with core-crossing trajectories is visible at high energies. The trigger applied here looks for events with pulses on at least 3 PMTs within a 10 ns window. The current simulated test geometry has an effective area at trigger level comparable to that of the IceCube detector, as expected based on their comparable geometric volumes. [19].

provide a view of the sky complementary to existing and planned neutrino telescopes in Antarctica, the Mediterranean, Lake Baikal and the western Pacific.

Acknowledgments

We thank Ocean Networks Canada for the very successful operation of the NEPTUNE observatory, as well as the support staff from our institutions without whom P-ONE could not be operated efficiently.

We acknowledge the support of Natural Sciences and Engineering Research Council, Canada Foundation for Innovation, Digital Research Alliance, and the Canada First Research Excellence Fund through the Arthur B. McDonald Canadian Astroparticle Physics Research Institute, Canada; European Research Council (ERC), European Union; Deutsche Forschungsgemeinschaft (DFG), Germany; National Science Centre, Poland; U.S. National Science Foundation-Physics Division, USA.

References

[1] M. Agostini *et al. Nature Astronomy* **4** no. 10, (2020) 913–915.

[2] M. G. Aartsen *et al. Journal of Instrumentation* **12** no. 03, (2017) P03012.

[3] S. Adrian-Martinez *et al. Journal of Physics G: Nuclear and Particle Physics* **43** no. 8, (2016) 084001.

[4] K. Holzapfel *et al.*, "Pathfinders of the Pacific Ocean Neutrino Experiment," in *PoS ICRC2023*. 2023. (these proceedings).

[5] M. Boehmer *et al.*, "Sub-ns timing for the Pacific Ocean Neutrino Experiment by optical fiber using Gigabit Ethernet," in *PoS ICRC2023*. 2023. (these proceedings).

[6] C. Haack, L. Schumacher, *et al.*, "Machine-learning aided detector optimization of the Pacific Ocean Neutrino Experiment," in *PoS ICRC2023*. 2023. (these proceedings).

[7] C. Spannfellner *et al.*, "Development of the first detector line of the Pacific Ocean Neutrino Experiment," in *PoS ICRC2023*. 2023. (these proceedings).

[8] "GitHub - icecube/icetray-public: Public subset of IceTray — github.com." https://github.com/icecube/icetray-public. [Accessed 13-Jul-2023].

[9] R. Abbasi *et al. Computer Physics Communications* **266** (2021) 108018.

[10] J.-M. Alameddine *et al.*, "Proposal: A library to propagate leptons and high energy photons," in *Journal of Physics: Conference Series*, vol. 1690, p. 012021, IOP Publishing. 2020.

[11] H. Schwanekamp *et al. Computing and Software for Big Science* **6** no. 1, (2022) 4.

[12] **AMANDA** Collaboration, J. Ahrens *et al. Nucl. Instrum. Meth. A* **524** (2004) 169–194.

[13] **IceCube** Collaboration, R. Abbasi *et al. Journal of Instrumentation* **16** no. 08, (2021) P08034.

[14] N. Whitehorn, J. van Santen, and S. Lafebre *Computer Physics Communications* **184** no. 9, (2013) 2214–2220.

[15] K. Schatto, *Stacked searches for high-energy neutrinos from blazars with IceCube*. PhD thesis, Mainz, Univ., Diss., 2014, 2014.

[16] M. G. Aartsen *et al. Nuclear Instruments and Methods in Physics Research A* **736** (Feb., 2014) 143–149.

[17] G. B. Dantzig, *Origins of the Simplex Method*, p. 141–151. Association for Computing Machinery, New York, NY, USA, 1990. https://doi.org/10.1145/87252.88081.

[18] "Tidbits x2014; Projects 0.1 documentation — user-web.icecube.wisc.edu." https://user-web.icecube.wisc.edu/~jvansanten/docs/misc/index.html#weighting-tricks. [Accessed 13-Jul-2023].

[19] A. Karle *arXiv:1003.5715* (2010) .

Full Authors List: P-ONE Collaboration

Matteo Agostini[11], Nicolai Bailly[1], A.J. Baron[1], Jeannette Bedard[1], Chiara Bellenghi[2], Michael Böhmer[2], Cassandra Bosma[1], Dirk Brussow[1], Ken Clark[3], Beatrice Crudele[11], Matthias Danninger[4], Fabio De Leo[1], Nathan Deis[1], Tyce DeYoung[6], Martin Dinkel[2], Jeanne Garriz[6], Andreas Gärtner[5], Roman Gernhäuser[2], Dilraj Ghuman[4], Vincent Gousy-Leblanc[2], Darren Grant[6], Christian Haack[14], Robert Halliday[6], Patrick Hatch[3], Felix Henningsen[4], Kilian Holzapfel[2], Reyna Jenkyns[1], Tobias Kerscher[2], Shane Kerschtien[1], Konrad Kopański[15], Claudio Kopper[14], Carsten B. Krauss[5], Ian Kulin[1], Naoko Kurahashi[12], Paul C. W. Lai[11], Tim Lavallee[1], Klaus Leismüller[2], Sally Leys[8], Ruohan Li[2], Paweł Malecki[15], Thomas McElroy[5], Adam Maunder[5], Jan Michel[9], Santiago Miro Trejo[5], Caleb Miller[4], Nathan Molberg[5], Roger Moore[5], Hans Niederhausen[6], Wojciech Noga[15], Laszlo Papp[2], Nahee Park[3], Meghan Paulson[1], Benoît Pirenne[1], Tom Qiu[1], Elisa Resconi[2], Niklas Retza[2], Sergio Rico Agreda[1], Steven Robertson[5], Albert Ruskey[1], Lisa Schumacher[14], Stephen Sclafani[12 α], Christian Spannfellner[2], Jakub Stacho[4], Ignacio Taboada[13], Andrii Terliuk[2], Matt Tradewell[1], Michael Traxler[10], Chun Fai Tung[13], Jean Pierre Twagirayezu[6], Braeden Veenstra[5], Seann Wagner[1], Christopher Weaver[6], Nathan Whitehorn[6], Kinwah Wu[11], Juan Pablo Yañez[5], Shiqi Yu[6], Yingsong Zheng[1]

[1]Ocean Networks Canada, University of Victoria, Victoria, British Columbia, Canada.
[2]Department of Physics, School of Natural Sciences, Technical University of Munich, Garching, Germany.
[3]Department of Physics, Engineering Physics and Astronomy, Queen's University, Kingston, Ontario, Canada.
[4]Department of Physics, Simon Fraser University, Burnaby, British Columbia, Canada.
[5]Department of Physics, University of Alberta, Edmonton, Alberta, Canada.
[6]Department of Physics and Astronomy, Michigan State University, East Lansing, MI, USA.
[8]Department of Biological Sciences, University of Alberta, Edmonton, Alberta, Canada.
[10]Gesellschaft für Schwerionenforschung, Darmstadt, Germany.
[11] Department of Physics and Astronomy and Mullard Space Science Laboratory, University College London, United Kingdom
[12] Department of Physics, Drexel University, 3141 Chestnut Street, Philadelphia, PA 19104, USA.
[13] School of Physics and Center for Relativistic Astrophysics, Georgia Institute of Technology, Atlanta, GA, USA.
[14] Erlangen Centre for Astroparticle Physics, Friedrich-Alexander-Universität Erlangen-Nürnberg, D-91058 Erlangen, Germany.
[15] H. Niewodniczański Institute of Nuclear Physics, Polish Academy of Sciences, Radzikowskiego 152, 31-342 Kraków, Poland.
$^{\alpha}$ now at Department of Physics, University of Maryland, College Park, MD 20742, USA.